Supporting Information

Constructing a novel strategy for controllable synthesis of corrosion resistant Ti^{3+} self-doped titanium-silicon materials with efficient hydrogen evolution activity from simulated seawater

Ting Song, Piyong Zhang, Tingting Wang, Atif Ali and Heping Zeng*

Key Laboratory of Functional Molecular Engineering of Guangdong Province, School of Chemistry and Chemical Engineering, South China University of Technology, Guangzhou 510641, P. R. China.

*****Corresponding author. Tel.: +86-20-87112631; Fax: +86-20-87112631; E-mail: hpzeng@scut.edu.cn;

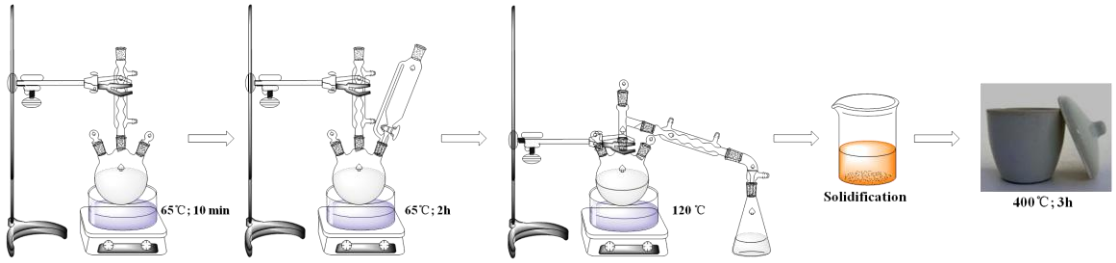

Figure S1. Detailed synthesis steps for the preparation of Ti-O-Si materials.

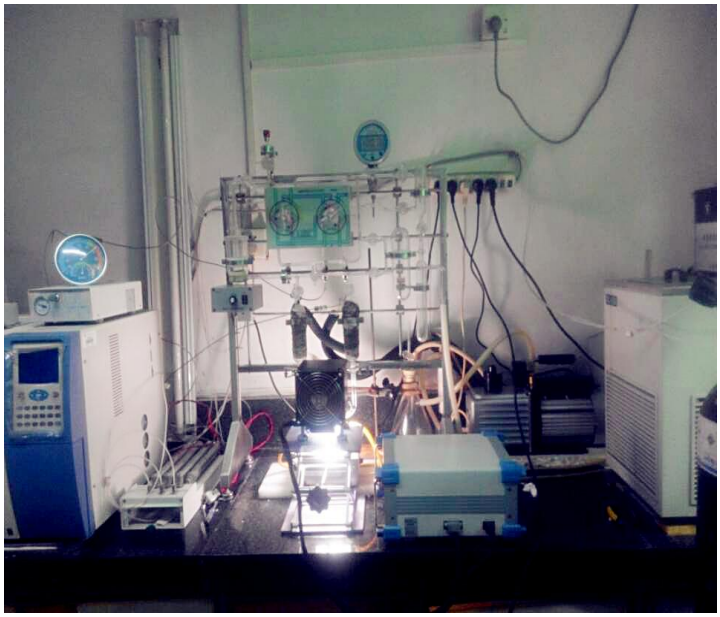

Figure S2. The photocatalytic H_2 production equipment with the gas chromatography (GC7900, Tian Mei, Shanghai) by nitrogen as a carrier gas.

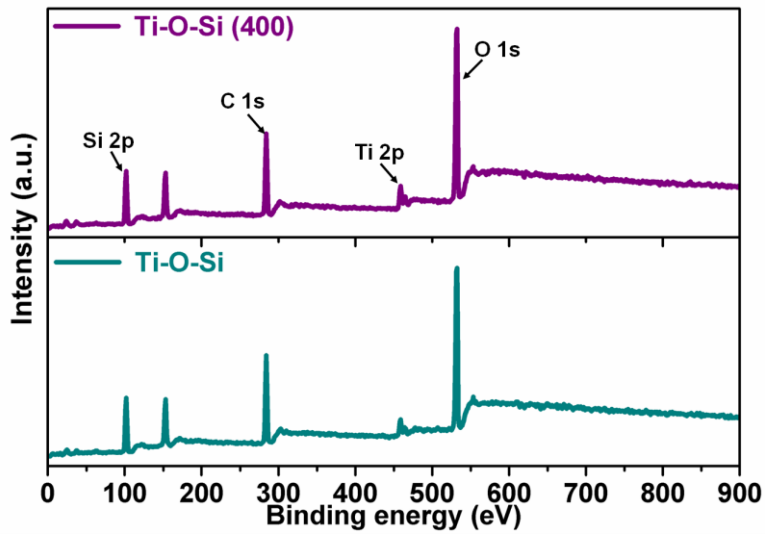

Figure S3. The full-scale XPS spectrum of Ti-O-Si and Ti-O-Si (400).

Table S1. Surface atomic concentration of Ti-O-Si (400) come from XPS.

Sample	**C 1s**	**O 1s**	**Si 2p**	**Ti^{4+}**	**Ti^{3+}**
Ti-O-Si	42.45	32.21	21.03	4.31	0
Ti-O-Si (400)	42.16	32.94	20.68	4.07	0.15

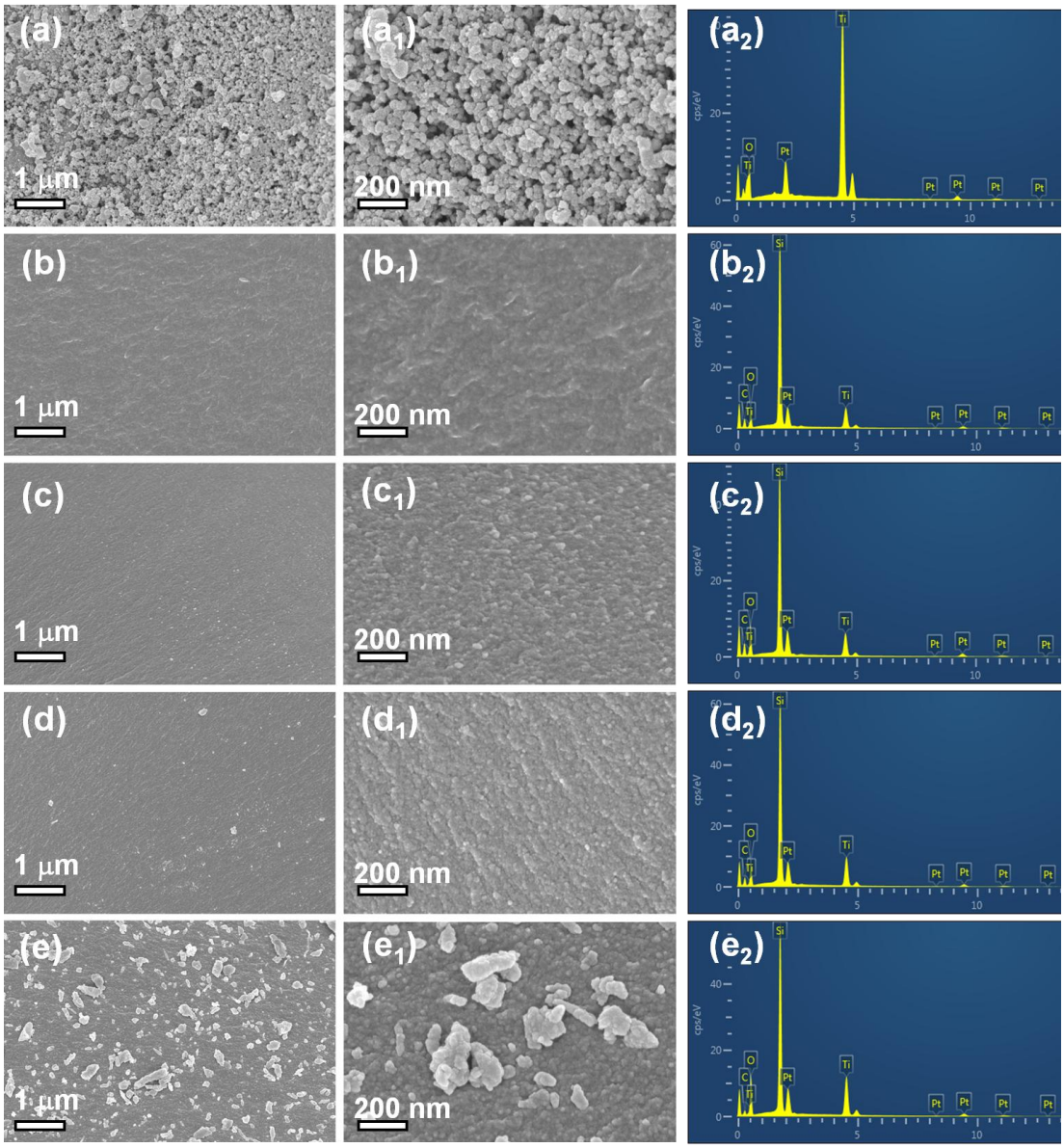

Figure S4. SEM images of the as-prepared composites: TiO_2 ((a), (a_1)), Ti-O-Si ((b), (b_1)), Ti-O-Si (400) ((c), (c_1)), Ti-O-Si (500) ((d), (d_1)), and Ti-O-Si (600) ((e), (e_1)); EDS spectrum of TiO_2 (a_2), Ti-O-Si (b_2), Ti-O-Si (400) (c_2), Ti-O-Si (500) (d_2), and Ti-O-Si (600) (e_2).

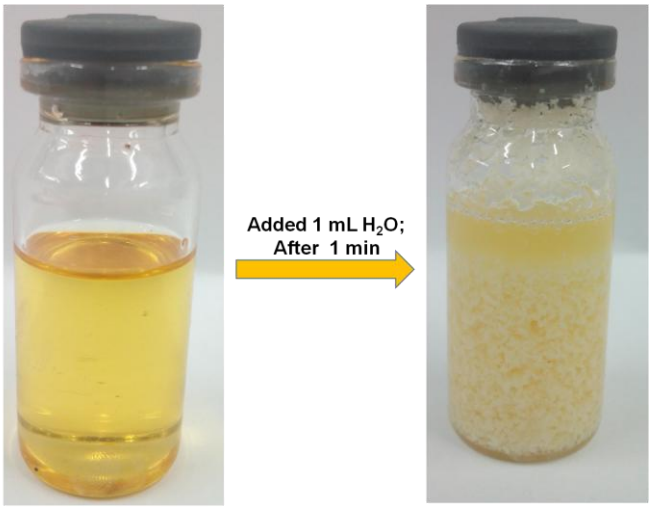

Figure S5. After 1 min, pure etrabutyl titanate sample becomes turbid with dropping 1.0 mL of water.

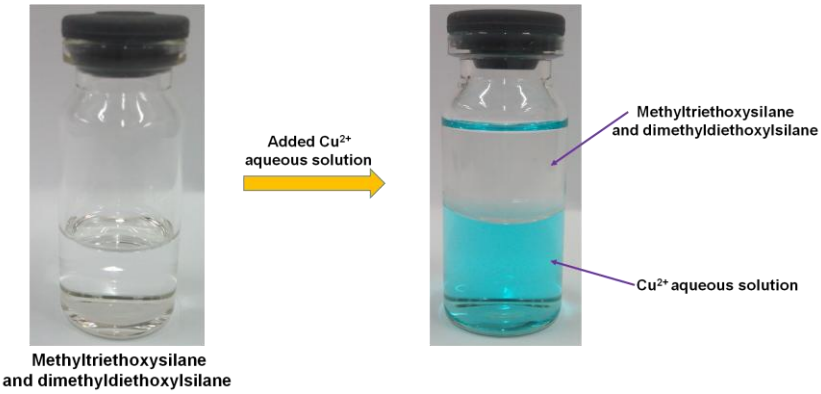

Figure S6. The mixed solution of methyltriethoxysilane and dimethyldiethoxylsilane is not soluble in water.

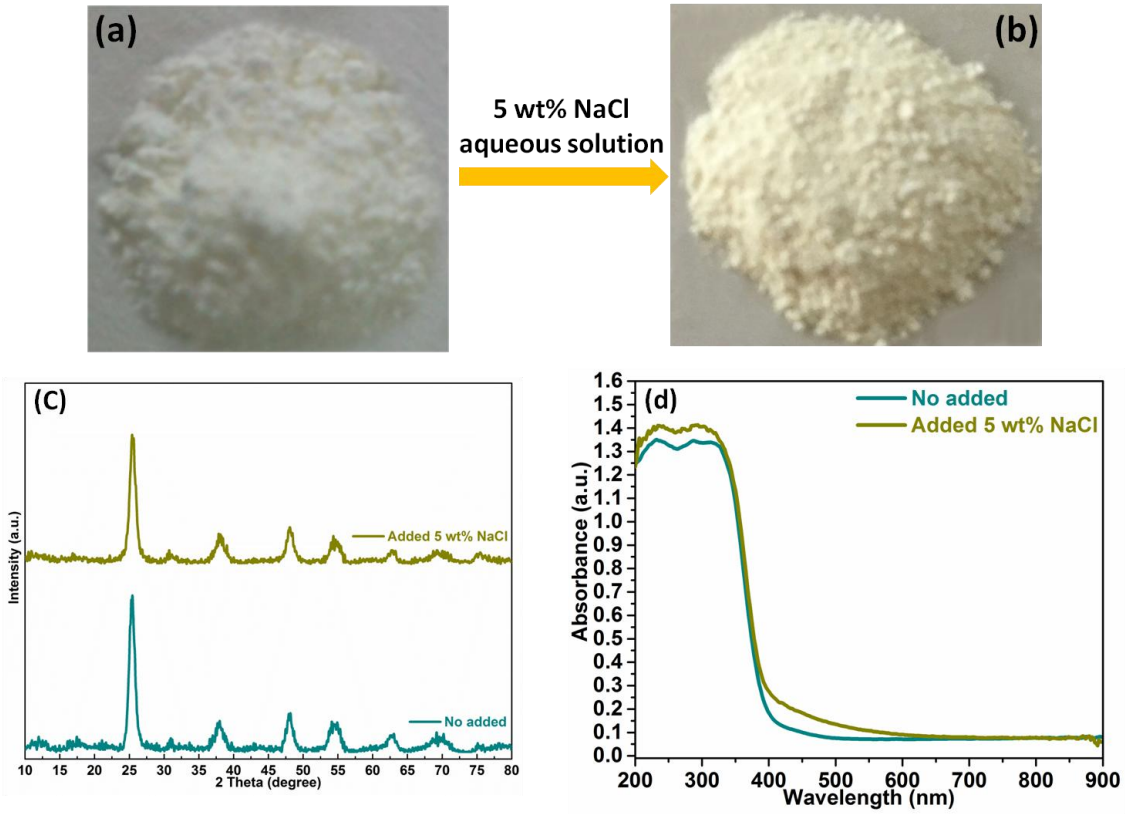

Figure S7. Sample pictures of TiO_2 nanoparticles without (a) and with added 5 wt% NaCl aqueous solution (b). The TiO_2 nanoparticles were soaked in 5 wt% NaCl aqueous solution for about 10 days. XRD patterns (c) and UV-vis diffuse reflectance spectra (d) of TiO_2 nanoparticles without and with added 5 wt% NaCl aqueous solution.

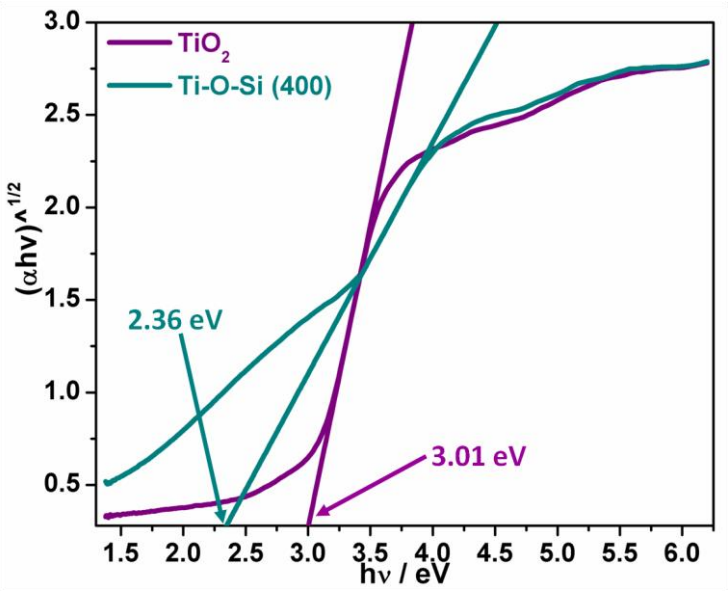
TiO2
Ti-O-Si (400)
2.36 eV
3.01 eV
(αhν)^1/2
hν / eV

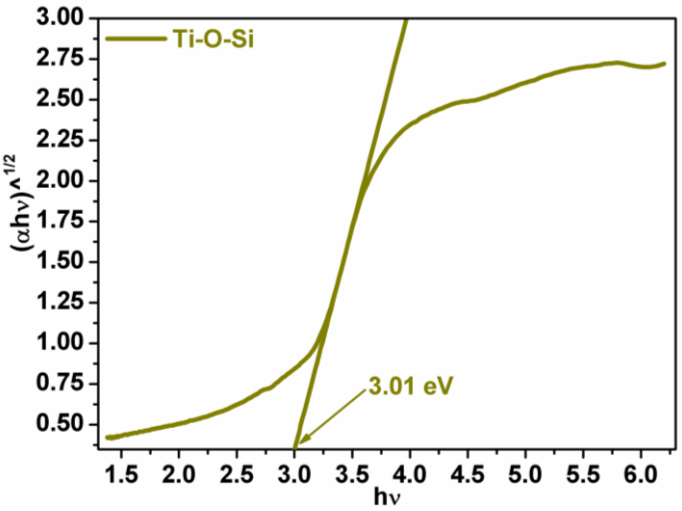
Ti-O-Si
3.01 eV
(αhν)^1/2
hν

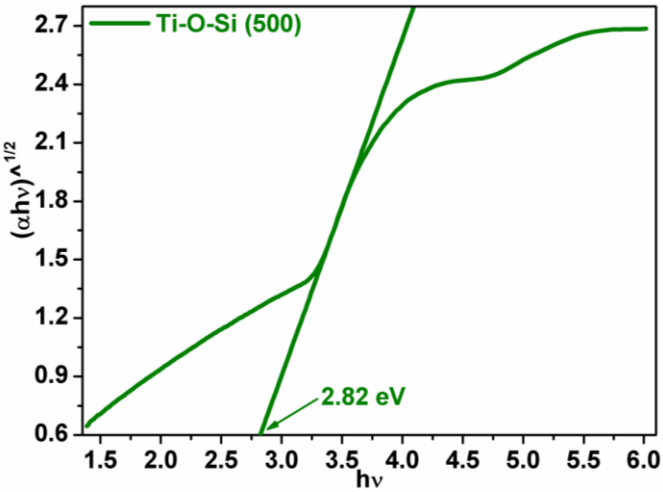
Ti-O-Si (500)
2.82 eV
(αhν)^1/2
hν

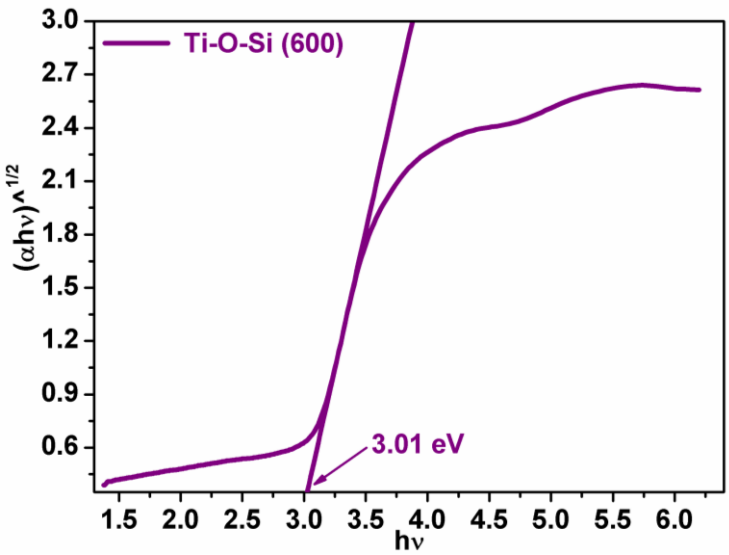

Figure S8. The $(\alpha h\nu)^{1/2}$ versus hv curve of TiO_2, Ti-O-Si, Ti-O-Si (400), Ti-O-Si (500), and Ti-O-Si (600); The band structure of the compounds are calculated by the KubelKa-Munk (KM) method according to the following equation: $\alpha h\nu=A(h\nu-Eg)^2$, where α is the absorption coefficient, hv is the photo energy, Eg is the direct band gap, and A is a constant.

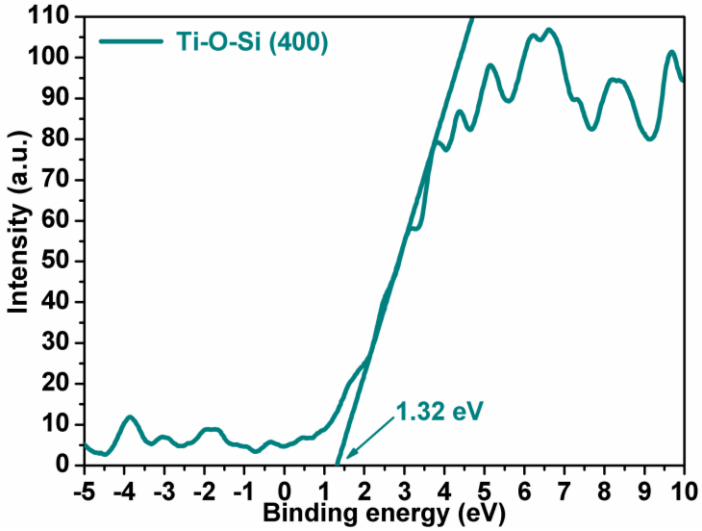

Figure S9. The VB XPS of Ti-O-Si (400).

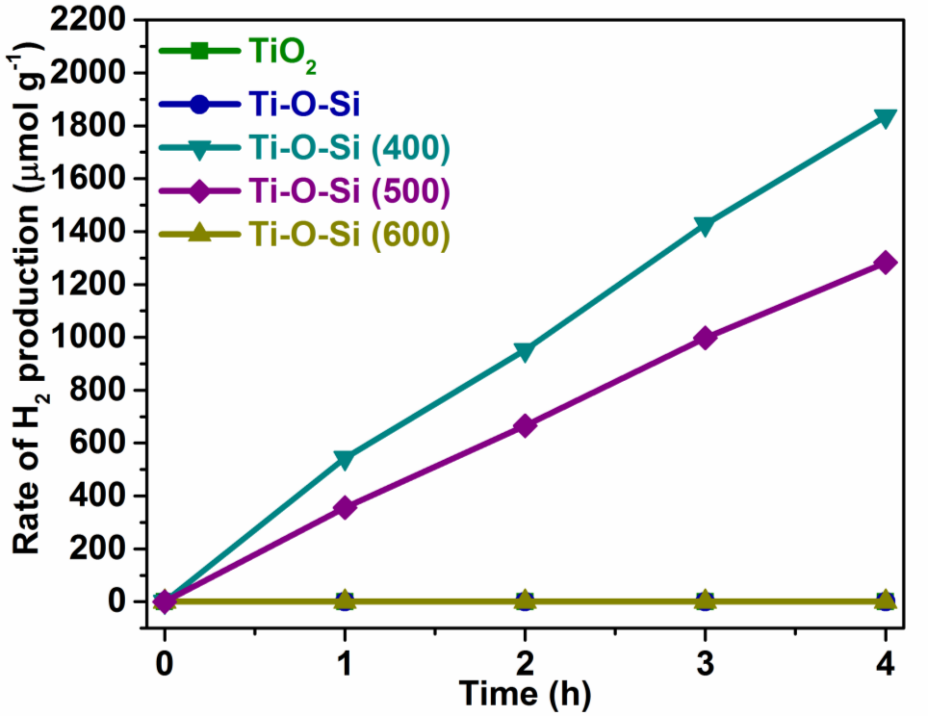

Figure S10. Photocatalytic activity of the investigated samples in an aqueous solution under visible light irradiation (λ>420 nm) containing 10 vol% TEOA adjusted to pH 8.2 with add 5 wt% NaCl ((vs 70 mL water).

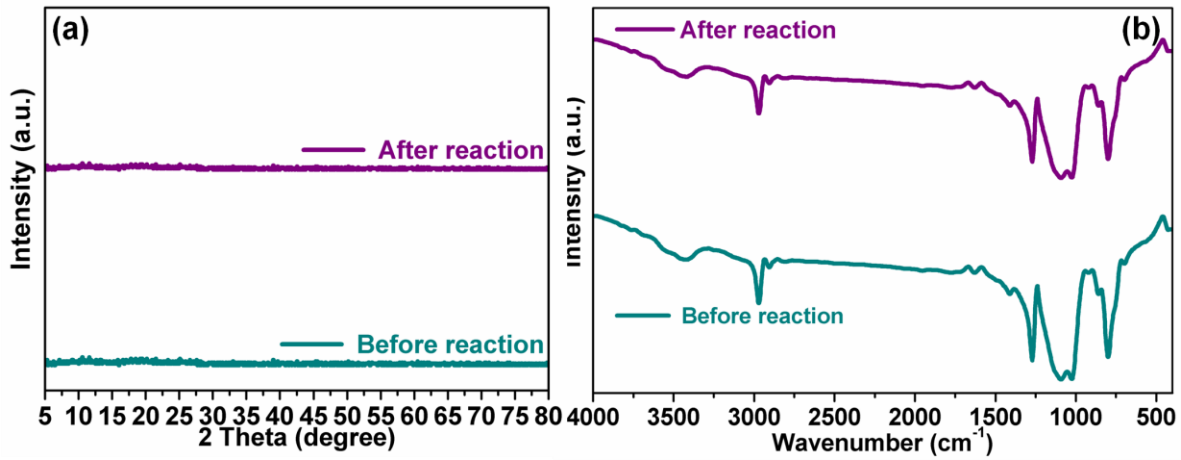

Figure S11. XRD patterns (a) and FTIR spectra (b) of Ti-O-Si (400) composite before and after the stability test.

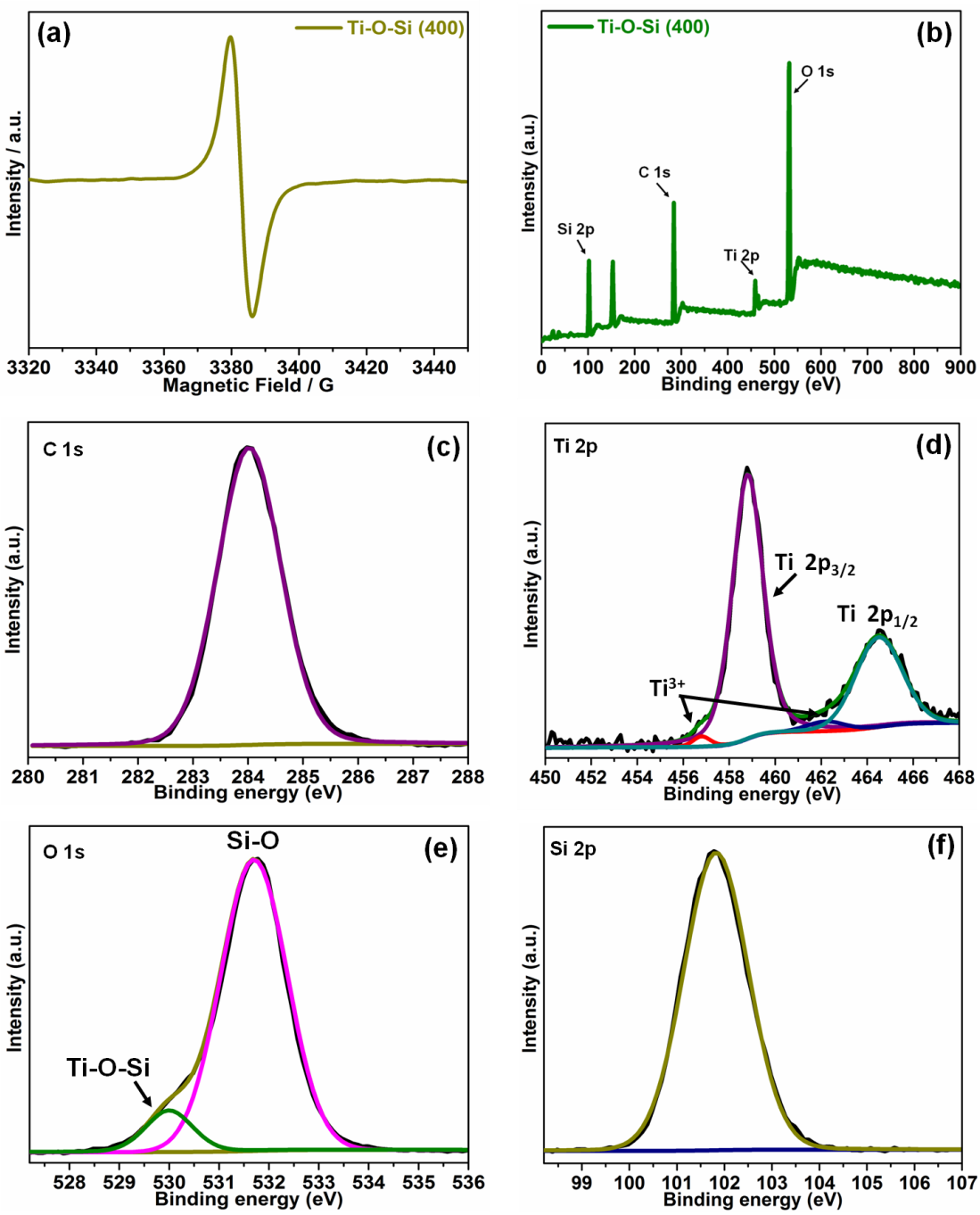

Figure S12. (a) EPR spectrum of Ti-O-Si (400) at 110 K after the stability test. XPS analysis of the Ti-O-Si (400) composite after the stability test. The full-scale XPS spectrum (b), High resolution XPS spectra of C 1s (c), Ti 2p (d), O 1s (e), and Si 2p (f), respectively.

The apparent Quantum Efficiency Measurement

The apparent quantum efficiency (AQE) was measured using the same experimental setup for the photocatalytic hydrogen evolution, but with an additional band-pass filter to obtain monochromatic light. Band-pass filters (420 nm) were equipped when conducting reactions under photons of different wavelengths and collecting quantum efficiency (QE) results. The amount of H_2 produced in the first 10 h was used to calculate quantum efficiency using the equation below. The average intensity of irradiation was determined to be 3.15 $mW \cdot cm^{-2}$ and the irradiation area was 13.3 cm^2. The amount of H_2 molecules generated in 10 hours for Ti-O-Si (400) were 235.67 μmol. The quantum efficiency was calculated by Equation 1.

$$AQE = \frac{2 \times \text{the number of evolved hydrogen molecules}}{\text{the number of incident photons}} \times 100\%$$

Number of H_2 molecules = $6.02 \times 10^{23} \times 235.67 \times 10^{-6} = 1.419 \times 10^{20}$

Number of incident photons = $E\lambda/hc = (3.15 \times 10^{-3} \times 13.3 \times 3600 \times 10 \times 420 \times 10^{-9}) / (6.626 \times 10^{-34} \times 3 \times 10^{8}) = 3.187 \times 10^{21}$

The calculated AQE for Ti-O-Si (400) at 420 nm is 8.9 %.

Table S2. The comparation of photocatalytic H_2 production activity among Ti^{3+} self-doped TiO_2 materials reported in the literatures over recent years and **this work**.

Photocatalyst	Reducing agent	Reaction conditions	Application	Ehancement fators vs. No Ti^{3+} (The same condition)	Sample picture
Black TiO_2 nanotube arrays [S1]	Al	500 °C for 4 h; Base pressure below 8 Pa;	Photoelectro chemical Water-Splitting **(freshwater)**	1.20%	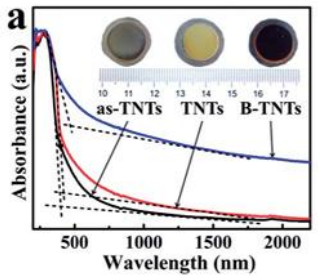
Hydrogen treated anatase TiO_2 [S2]	H_2	300 °C for 10, 20 and 30 h; 5% H_2 balanced Ar; Chamber pressure at 2×10^{-2} Torr.	photodegrade MB	three orders of magnitude	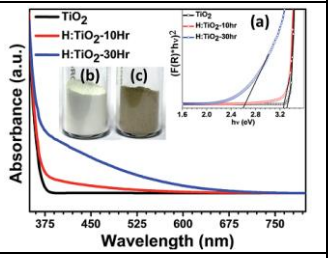
Oxygen-deficient TiO_2 nanocrystals [S3]	$NaBH_4$	Ar atmosphere at 300 °C for 30 min.	CO_2 Photoreduction	12.4	No picture
3D mesoporous black $TiO_2/MoS_2/TiO_2$ nanosheets [S4]	$NaBH_4$	350°C for 1 h under an Ar atmosphere	Photocatalytic hydrogen evolution **(freshwater)**	0.56 μmol h^{-1} g^{-1}	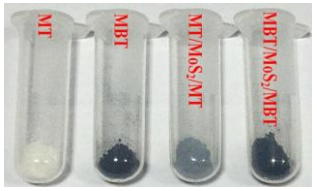
Black TiO_2 foams [S5]	H_2	At 600 °C for 3 h	Photodegrade hexadecane	7 times	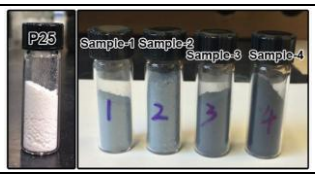
Black TiO_x nanoparticles [S6]	Mg	At 500, 600, and 700 °C under an Ar atmosphere for 4 h	Solar Water Evaporation	50%	No picture
3D flower-like black N-TiO_{2-x}@ MoS_2 [S7]	$NaBH_4$	350 °C for 2 h under the Ar atmosphere	Photocatalytic hydrogen evolution **(freshwater)**	1.882 mmol h^{-1} g^{-1}	No picture

Black titania nanobelts [S8]	Al	Pressure of ~2 Pa; At 550 °C for 4.5 h.	Oxygen-Reduction Activity **(freshwater)**	5.7 mA cm^{-2}	No picture
Core-shelled black anatase titania [S9]	urea	550 °C for 3 h; Under the N_2 atmosphere	Decomposition of methyl orange (MO)	53.77%	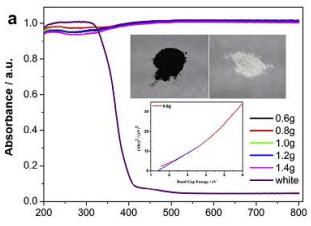
Mesoporous black TiO_2 hollow spheres [S10]	H_2	At 600 °C for 3 h under normal pressure conditions	Photocatalytic hydrogen evolution **(freshwater)**	241 μmol h^{-1} 0.1 g^{-1}	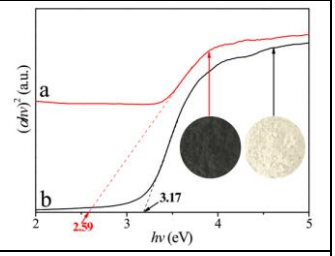
Ti^{3+} in anatase TiO_2 [S11]	$NaBH_4$	Solvothermally treated at 180 °C for 24 h	Photodegrade MB	30-fold	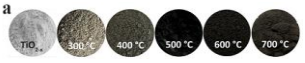
$SrTiO_{3-x}/TiO_{2-x}$ [S12]	Al	450 °C ($SrTiO_3/TiO_2$) for 6 h in a 5×10^{-4} Pa pressure	photoelectrochemical hydrogen production	40 times	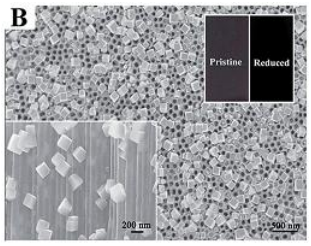
Reduced rutile TiO_2 [S13]	No added	Ar^+ sputtering and UHV annealing at 850 K	photocatalytic activity	No data	No picture
Black TiO_2 nanotubes [S14]	H_2	At 20 bar at 500 °C for 1 h.	Photocatalytic hydrogen evolution **(freshwater)**	7 μmol/(h cm^2)	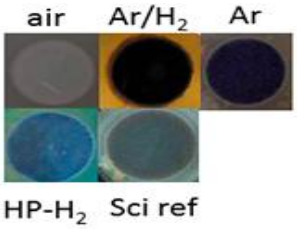
Corrosion resistant Ti^{3+} self-doped Ti-O-Si material (This work)	No reducing agent	At 400 °C for 3 h; Atmospheric and air atmosphere	Photocatalytic hydrogen evolution (**Freshwater** or **simulated seawater**)	**1640.2** or **1930.5** μmol h^{-1} g^{-1}	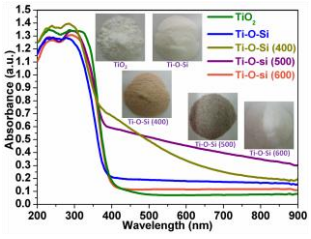

References:

1. H. L. Cui, W. Zhao, C. Y. Yang, H. Yin, T. Q. Lin, Y. F. Shan, Y. Xie, H. Gua and F. Q. Huang, *J. Mater. Chem. A*, 2014, **2**, 8612-8617.

2. M. Mehta, N. Kodan, S. Kumar, A. Kaushal, L. Mayrhofer, M. Walter, M. Moseler, A. Dey, S. Krishnamurthy, S. Basu and A. P. Singh, *J. Mater. Chem. A*, 2016, **4**, 2670-2681.

3. L. J. Liu, Y. Q. Jiang, H. L. Zhao, J. T. Chen, J. L. Cheng, K. S. Yang and Y. Li, *ACS Catal*., 2016, **6**, 1097-1108.

4. X. F. Liu, Z. P. Xing, H. Zhang, W. M. Wang, Y. Zhang, Z. Z. Li, X. Y. Wu, X. J. Yu and W. Zhou, *ChemSusChem*, 2016, **9**, 1118-1124.

5. K. F. Zhang, W. Zhou, X. C. Zhang, B. J. Sun, L. Wang, K. Pan, B. J. Jiang, G. H. Tian and H. G. Fu, *Appl. Catal. B: Environ.*, 2017, **206**, 336-343.

6. M. M. Ye, J. Jia, Z. J. Wu, C. X. Qian, R. Chen, P. G. O'Brien, W. Sun, Y. C. Dong and G. A. Ozin, *Adv. Energy Mater*., 2017, **7**, 1601811-1601818.

7. X. F. Liu, Z. P. Xing, Y. Zhang, Z. Z. Li, X. Y. Wu, S. Y. Tan, X. J. Yu, Q. Zhu, W. Zhou, *Appl. Catal. B: Environ*., 2017, **201**, 119-127.

8. X. T. Yuan, X. Wang, X. Y. Liu, H. X. Ge, G. H. Yin, C. L. Dong and F. Q. Huang, *ACS Appl. Mater. Interfaces*, 2016, **8**, 27654-27660.

9. S. H. Wei, R. Wu, X. X. Xu, J. K. Jian, H. X. Wang, Y. F. Sun, *Chem. Eng. J*., 2016, **299**, 120-125.

10. W. Y. Hu, W. Zhou, K. F. Zhang, X. C. Zhang, L. Wang, B. J. Jiang, G. H. Tian, D. Y. Zhao and H. G. Fu, *J. Mater. Chem. A*, 2016, **4**, 7495-7502.

11. X. Y. Xin, T. Xu, J. Yin, L. Wang, C. Y. Wang, *Appl. Catal. B: Environ*., 2015, **176**, 354-362.

12. M. D. Shang, H. Y. Hu, G. X. Lu and Y. P. Bi, *J. Mater. Chem. A*, 2016, **4**, 5849-5853.

13. Z. Q. Wang, B. Wen, Q. Q. Hao, L. M. Liu, C. Y. Zhou, X. C. Mao, X. F. Lang, W. J. Yin, D. X. Dai, A. Selloni and X. M. Yang, *J. Am. Chem. Soc*., 2015, **137**, 9146-9152.

14. N. Liu, C. Schneider, D. Freitag, M. Hartmann, U. Venkatesan, J. Müller, E. Spiecker and P. Schmuki, *Nano Lett*., 2014, **14**, 3309-3313.